ELSEVIER

0144-8617(94)00050-6

Carbohydrate Polymers **25** (1994) 177–185

0144-8617/94/$07.00

Static light scattering technique applied to pectin in dilute solution. Part I: Reliability of experiments and model calculations

Gisela Berth,[a*†] Herbert Dautzenberg[b] & Gudrun Rother[b]

[a]*Deutsches Institut für Ernährungsforschung Potsdam-Rehbrücke, Arthur-Scheunert-Allee 114–116, D-14558 Bergholz-Rehbrücke, Germany*
[b]*Max-Planck-Institut für Kolloid- und Grenzflächenforschung Teltow, Kantstr. 55, D-14513 Teltow-Seehof, Germany*

(Received 22 June 1993; accepted 7 February 1994)

During static light scattering studies of a commercial high-methoxyl citrus pectin in phosphate buffer, problems arising from sample clarification have been identified. Therefore, the effect of varying the pore size of the membrane filters between 5·0 and 0·2 μm was studied. Also, the effect of repeated filtration was investigated. Data are presented as Zimm and Guinier plots. The lower the pore size of the filter, the lower the average molecular weight, but the higher the negative second virial coefficients found. Results suggest that the negative virial coefficients are due to residual particulate matter. Model calculations suggest that a bimodal system consisting of a molecularly dispersed major component and smaller amounts of a high molecular weight particulate component is an appropriate description of the pectin sample. Dextran sulphate was used to demonstrate the behaviour of a 'homogeneous' non-aggregating polysaccharide.

INTRODUCTION

Light scattering studies on (ionic) polysaccharides are known to be difficult. The common double extrapolation to zero concentration and zero angle, according to Zimm (1948) often gives plots which differ strongly from the expected 'ideal' shape. The conventional interpretation of these data in terms of the weight average molecular weight M_W, the root of the z-average of the square of the radius of gyration $\langle s^2 \rangle^{1/2}$, and the second virial coefficient B (e.g. Huglin, 1972) appears not to be advisable.

At least in part, confusion comes from the unexpectedly small positive or often negative B values. For pectins these values are in contradiction to what have been obtained by other techniques such as sedimentation analysis (Säverborn, 1945; Devine, 1974; Harding & Horton, pers. comm.) or membrane osmometry (Pals & Hermans, 1952; Berth, unpublished).

The general theory of macromolecular solution behaviour shows that negative virial coefficients can be indicative of a concentration dependent association/dissociation. In that case, the formation or breakdown of high-molecular weight aggregates should produce characteristic effects on the angular dependence of the scattered light, and hence the shape of the scattering function $P(\theta)$. However, the extremely small and even negative virial coefficients observed in light scattering measurements can also be the consequence of some residual high-molecular particulate matter in a molecularly dispersed surrounding.

Whereas many polysaccharides are not prone to self-association at low concentrations, it seems to be the rule rather than the exception that their solutions contain some particulate matter (Berth, 1992). If these particles—which can be both extraneous material and part of the substance under study—are large and/or have a high density compared with the molecularly dispersed subject of interest, they can be easily and completely removed by filtration and centrifugation, permitting an undistorted characterization of the remaining solution. The process of preparing optically clean solutions is called 'clarifica-

*To whom correspondence should be addressed.
†Present address: Institute of Biotechnology, University of Trondheim, N-7034 Trondheim, Norway.

tion'. In other cases '... part of the difficulty of solution clarification arises from the overlapping dispersities of the properties (size, density, ...) of the polymers and the extraneous material' (Tabor, 1972). Pectins appear to belong to the latter type and there are reasons for considering that the particulate matter is not an impurity (Berth, 1988). Separate studies on the effects of concentration on the scattering from pectin samples by LALLS (Hourdet & Muller, 1991) and of the pore size of the membrane filter used for clarification prior to MALLS (Berth, 1992) have already shown the formidable effect of the clarification conditions chosen.

This paper is one of a series which is intended to summarize some recent experimental experience of light scattering studies on pectin. These observations might equally well apply to other heterogeneous polysaccharides with broad and more or less continuous size and density distributions of species.

The following experimental data were obtained on a commercial high-methoxyl citrus pectin which has already served as a model substance (Berth, 1988; Berth *et al.*, 1990; Berth & Lexow, 1991; Harding *et al.*, 1991). A critical survey on all manipulations involved in a typical light scattering measurement seems to be reasonable. A commercial dextran sulphate was used to demonstrate the light scattering behaviour of a polymer where the results are not sensitive to the methods of clarification.

Finally, we present some model calculations for illustrating the effect of small amounts of high-molecular weight matter in the presence of a molecularly dispersed polymer. This is intended to support the conclusions drawn from the experimental studies.

EXPERIMENTAL

Citrus pectin used was a commercial product from Koch-Light, UK, with a degree of esterification of *c.* 70%. Dextran sulphate was produced by Pharmacia (Sweden). Solutions were prepared at room temperature by stirring overnight in 0·037 M phosphate buffer of pH 6·5 with an addition of 1 mM l^{-1} disodium salt of EDTA. The pH value was adjusted by mixing equimolar solutions of Na_2HPO_4 and KH_2PO_4.

All membrane filters used were from Sartorius-Membranfilter (Göttingen, Germany) products, and made from cellulose nitrate.

Light scattering measurements were carried out using a 'Sofica' photogoniometer (FICA, France) equipped with a helium/neon laser of $\lambda = 632{\cdot}2$ nm (Zeiss Jena, Germany, or Uniphase, Germany) as a light source. All scattering intensities (measured at 11 or 31 positions between 30 and 150°) are related to the buffer purified under the same conditions. Pectin concentrations are related to the total carbohydrate determined by refractive index measurements (differential refractometer from Knauer, Germany). All symbols have their usual meaning (Huglin, 1972).

RESULTS AND DISCUSSION

Experimental investigations

Light scattering studies normally cover a broader concentration range in order to permit the extrapolation from real to ideal conditions. For that purpose it has become common practice to add successive filtered aliquots of the stock solution to the blank solvent in the measuring cell (see, e.g. Hourdet & Muller, 1991) or to prepare a concentration series by diluting a prepurified stock solution. To remove dust, etc., these solutions are pressed through a membrane filter of defined pore size directly into the measuring cells beginning with the pure solvent as the blank followed by the polymer solutions in order of increasing concentration (see also Tabor, 1972).

Usually the measured scattering intensities are plotted according to Zimm (1948). This method of data presentation is based on the equation:

$$\frac{K \cdot c}{R_\theta} = \frac{1}{M_W \cdot P(\theta)} + 2Bc + 3Cc^2 + \ldots \qquad (1)$$

where c is the polymer concentration in g ml^{-1}, M_W the weight average molecular weight, and B and C the second and third virial coefficients, respectively. R_θ is the Rayleigh ratio of the measured excess of intensity of the solution over that of the pure solvent (blank), $P(\theta)$ is the particle scattering function, and θ the scattering angle (e.g. see Evans, 1972). In the case of vertically polarized incident light, the optical constant K is given by

$$K = \frac{4\pi^2 \cdot n_0^2 \cdot \left(\frac{\partial n}{\partial c}\right)^2}{\lambda_0^4 \cdot N_a}, \qquad (2)$$

where n_0 is the refractive index of the solvent, $\partial n/\partial c$ is the specific refractive index increment of the polymer/solvent system measured at dialysis equilibrium, λ_0 is the wavelength of the light source *in vacuo*, and N_a is Avogadro's number. $1/P(\theta)$ can be expressed in the form:

$$P^{-1}(\theta) = 1 + \frac{16\pi^2}{3\lambda^2}\langle s^2\rangle_z \sin^2\frac{\theta}{2}, \qquad (3)$$

and provides, together with eqn (1), the following equation:

$$\frac{Kc}{R_\theta} = \frac{1}{M_W}\left[1 + \frac{16\pi^2}{3\lambda^2}\langle s^2\rangle_z \sin^2\frac{\theta}{2}\right] + 2Bc + 3Cc^2 + \ldots, \qquad (4)$$

where $\langle s^2\rangle_z$ stands for the z-average of the square of the radius of gyration.

The Zimm procedure involves plotting $K \cdot c/R_\theta$ versus $\sin^2(\theta/2) + kc$ (k is an arbitrary constant) and allows a double extrapolation to zero concentration and zero angle. The extrapolated points at different angles for the zero concentration are extrapolated to zero angle, and similarly the zero angle points at different concentrations are extrapolated to zero concentration. The two extrapolations should cut the $K \cdot c/R_\theta$ axis at the same point. The reciprocal of the intercept is equal to M_W, the initial slope of the concentration dependence at zero angle is equal to $2B$, and the initial slope of angular dependence at zero concentration yields $\langle s^2 \rangle_z^{1/2}$.

When this procedure is applied to citrus pectins clarified using membranes of pore sizes ranging from 5·0 down to 0·1 μm (covering the entire popular range) the series of Zimm plots shown in Fig. 1 is obtained. Apart from the fact that the quality of some measured points at low excess of scattering intensities is bad, the shape of the Zimm plots does not fit the generally expected ideal grid. Both the scattering intensities and the angular dependences were strongly reduced with smaller pore size. With increasing concentration the scattering curves became flatter and showed a significant downward trend. This is indicative of an increase in molecular

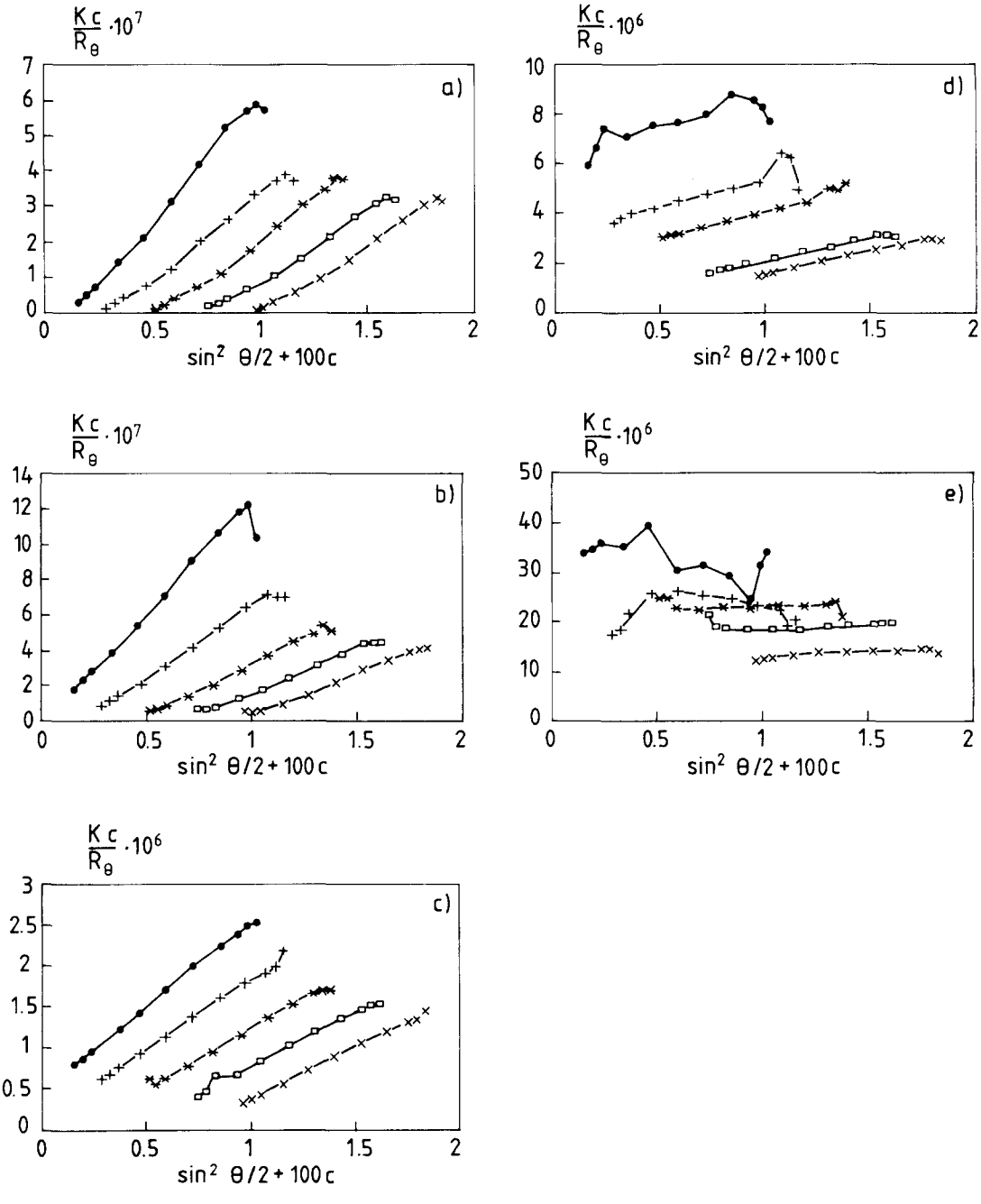

Fig. 1. Zimm plots for a citrus pectin concentration series after filtration through one filter each of different pore size in the order of increasing concentration (no rinsing steps); pore sizes: (a) 5·0 μm; (b) 0·8 μm; (c) 0·45 μm; (d) 0·2 μm; (e) 0·1 μm.

Table 1. Results of extrapolation from Fig. 1

Pore size (μm)	M_W	B (ml mol g^{-2})
5·0	$66{\cdot}7 \times 10^6$	$-3{\cdot}3 \times 10^{-5}$
0·8	$4{\cdot}0 \times 10^6$	$-9{\cdot}6 \times 10^{-5}$
0·45	$1{\cdot}0 \times 10^6$	$-1{\cdot}9 \times 10^{-4}$
0·2	66 000	$-5{\cdot}95 \times 10^{-3}$
0·1	31 250	n.d.

n.d. = not determined.

weight with concentration due to association since the molecular weight term in eqns (1) and (4) appears in the denominator. A rough analysis of these poor Zimm plots provides the results shown in Table 1. Therefore, molecular weights from *c.* 70 million down to about 30 000 are obtainable, depending on the pore size of the filter used. The lowest one is only one-third of the corresponding value from sedimentation analysis (Harding *et al.*, 1991) and even smaller than $M_n \sim 45\,000$ obtained from membrane osmometry (Berth *et al.*, 1990) on the same samples. This means that filters of pore sizes smaller than 0·45 μm have removed molecularly dispersed pectinaceous material. High molecular weights in Table 1 are associated with small negative B values. This is unexpected because higher molecular weight species should generally be formed in the *stronger* associating systems.

Figure 2 presents a collection of Zimm plots obtained when the same concentration series was filtered repeatedly through a 2 μm filter using a fresh filter for each plot. While the angular dependence appears to be only slightly altered, the scattering level was reduced with the number of filtration steps. Interpretation of the data, despite the large uncertainties in the extrapolation, gave the results shown in Table 2. According to these data the extrapolated molecular weight remains nearly constant ($M_W \sim 33\,000$) after the second filtration, but the negative B values are decreasing.

It should be mentioned that the membranes of 0·2 and in particular 0·1 μm pore size required a steadily increasing filtration pressure after the first few millilitres of filtrate had passed through. Obviously the pores become blocked, although we did not observe any 'slime' on the membrane surface as described by Smith (1976). However, filtration does lead to a measurable loss in carbohydrate matter. This was not taken into account here, but our further studies (Part II of this series) have shown that not more than 15% of the total polysaccharide disappears. On the other hand, the scattering intensities at 90° in Fig. 1 are reduced by a factor of 100 on progressive filtration through decreasing pore size filtres from 5 to 0·1 μm. Pretreatment of the stock solution or the concentration series by ultracentrifugation did not substantially improve the situation.

For a better understanding of the effects of filtration, we modified our procedure and filtered the concentration series in the order of decreasing concentration (blank first without rinsing between the different concentration levels). Whereas this somewhat curious practice made little difference to dextran sulphate (Fig. 3), the pectin sample reacted extremely sensitively as supermolecular structures containing systems usually do (e.g. see Kratochvil, 1972). The Zimm plot in Fig. 4(a), after the common procedure applied to a somewhat higher concentrated solution series, is in good accordance with Fig. 1. In contrast, Fig. 4(b) indicates the highest apparent molecular weight for the lowest concentration. This corresponds to the normal behaviour of well solvated polymers and is completely the opposite of what would be expected in the case of a concentration dependent association. The derivable second virial coefficient would acquire a positive B value and the molecular weight approaches infinity.

From all these data it is reasonable to assume the problem of light scattering measurements on pectins is due to the difficulty in clarifying an extremely heterogeneous material rather than association phenomena. However, a clear distinction cannot be made. Support in favour of one of these assumptions might be obtained from the angular dependence of the scattered light or, in other words, the scattering function $P(\theta)$. The most appropriate way of analysing this is in the form of a Guinier plot (Kerker, 1969). This is based upon the logarithmic reciprocal of eqn (1), which, when the concentration term is neglected, gives

$$\ln \frac{R_\theta}{K \cdot c} = \ln M_W + \ln P(\theta). \qquad (5)$$

Due to the decoupling of the molecular weight M_W and the scattering function $P(\theta)$, effects on the scattering level and the shape of the angular dependence can be separately assessed. Changes in the shape of the scattering function reflect changes in the dimensions, shape and polydispersities of the scatterers.

Guinier plots corresponding to Fig. 4(a) and (b) are given in Fig. 5, together with data taken from Fig. 2 (a)–(e) (the highest concentration for each) in order to demonstrate the effect of repeated filtration. For a more lucid presentation the curves were not shifted along the x-axis. It can be seen (Fig. 5(a) and (b)) that the scattering functions were only slightly changed by the filtration process whilst the scattering level depends strongly on the mode of filtration: the scattering curve of the lowest concentration is found on the bottom of Fig. 5(a), but lies on the top of Fig. 5(b). We have already pointed out that the amounts of polysaccharide involved in these effects are only small. They were too small to be indicated unambiguously by means of colorimetric methods, which work normally with an error not below ±5%. On the background of the largely unchanged angular dependencies these findings can be understood, assuming an increasing concentration or sample volume adsorption of high molecular weight

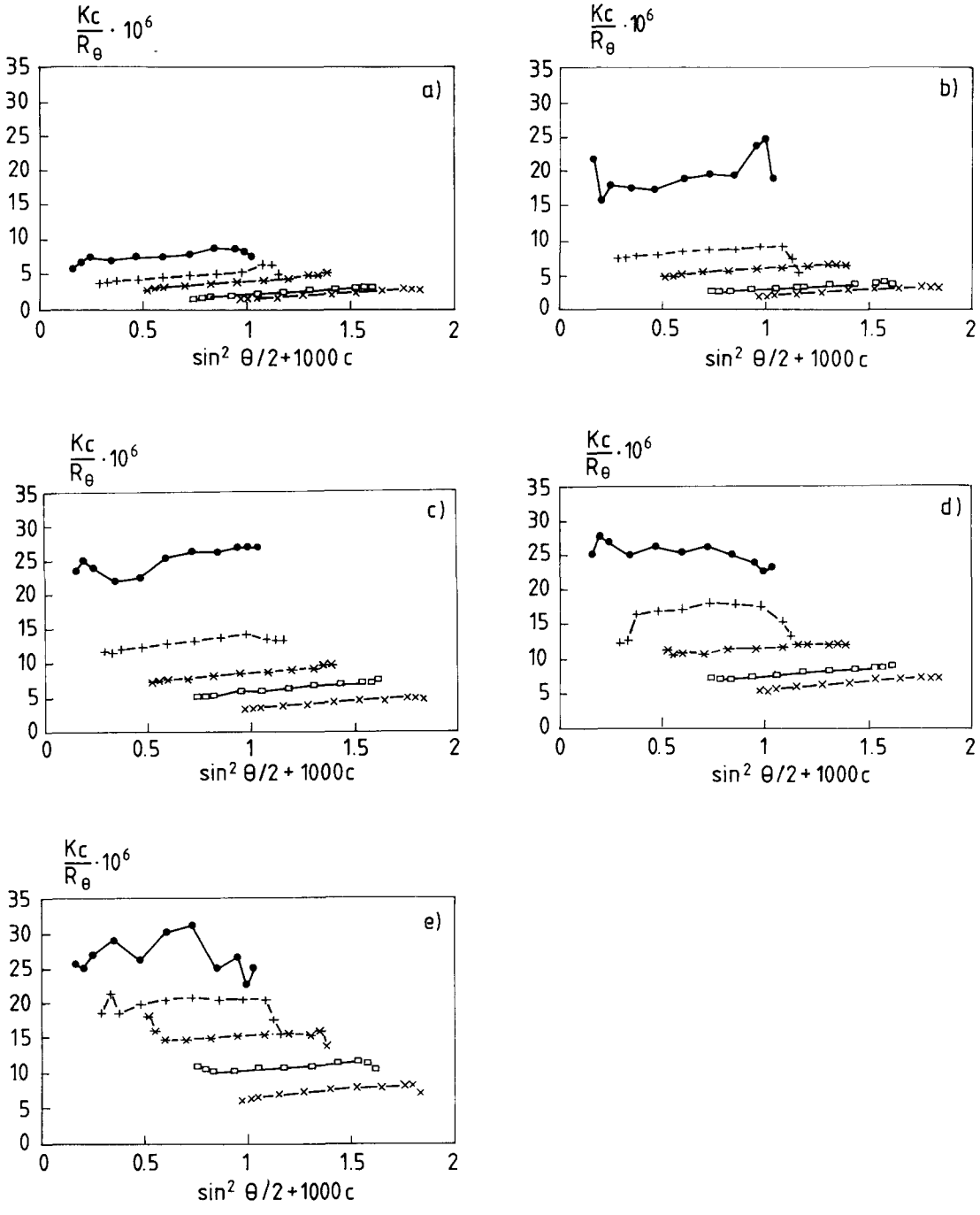

Fig. 2. Zimm plots obtained after repeated filtration of a citrus pectin concentration series using a fresh filter for each plot; pore size: 0·2 μm. (a) 1×; (b) 2×; (c) 3×; (d) 4×; (e) 5×.

carbohydrate on the filter and at least in part a desorption of previously retained matter when the filter is rinsed afterwards with more dilute solution.

Finally, Fig. 5(c) shows that repeated filtration causes both a reduction of the scattering level and a flattening of the scattering curves, which is indicative of the progressive removal of the largest species within the population.

Comparable effects were found using poly (vinyl chloride) filters, so that a specific interaction between the polymer and the membrane material can be excluded. Problems of clarification are obviously a consequence of the heterogeneity of the polymer itself. Description of the physical heterogeneity of commercial pectins on the basis of their chemical heterogeneity has been the subject of our previous papers. The complications arising from clarification make it difficult to address the issue of association in dilute pectin solutions at the moment. Also, from the theoretical point of view, there is the question as to how Zimm plots of the type shown above can be produced.

Table 2. Results of extrapolation from Fig. 2

Number of filtration steps	M_W	B (ml mol g^{-2})
1	66 000	$-5{\cdot}95 \times 10^{-3}$
2	33 300	$-1{\cdot}5 \times 10^{-2}$
3	33 300	$-6{\cdot}0 \times 10^{-3}$
4	33 300	$-4{\cdot}5 \times 10^{-3}$
5	33 300	$-4{\cdot}25 \times 10^{-3}$

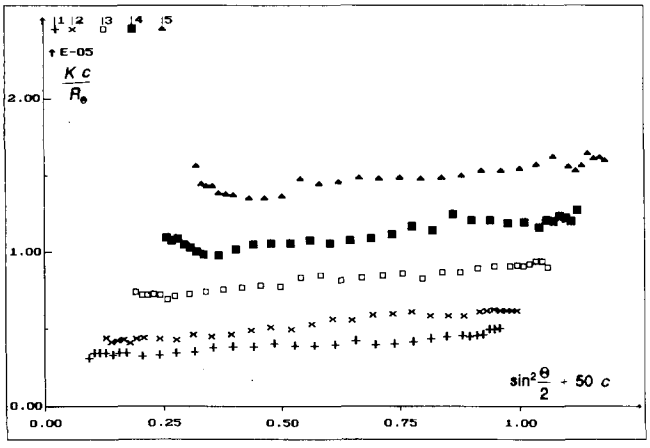

(a)

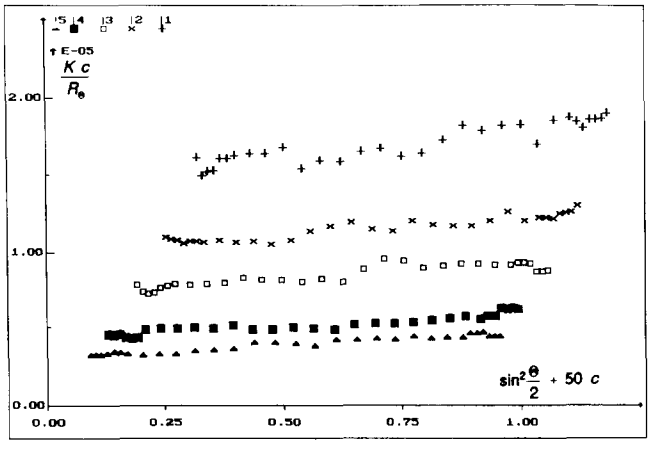

(b)

Fig. 3. Zimm plots obtained on dextran sulphate after filtering the concentration series in the order of (a) increasing and (b) decreasing concentration; pore size: 0·2 μm. M_W = 400 000.

Model calculations

The objective of this section is to show that the changes in the scattering behaviour due to filtration may be caused by a variation in the amount of the particulate component. For this purpose it is necessary to calculate the scattering curves of bimodal systems. Neglecting interactions between the molecularly dissolved and the particulate component as well as the non-ideality of the solution, scattering is described by the expression:

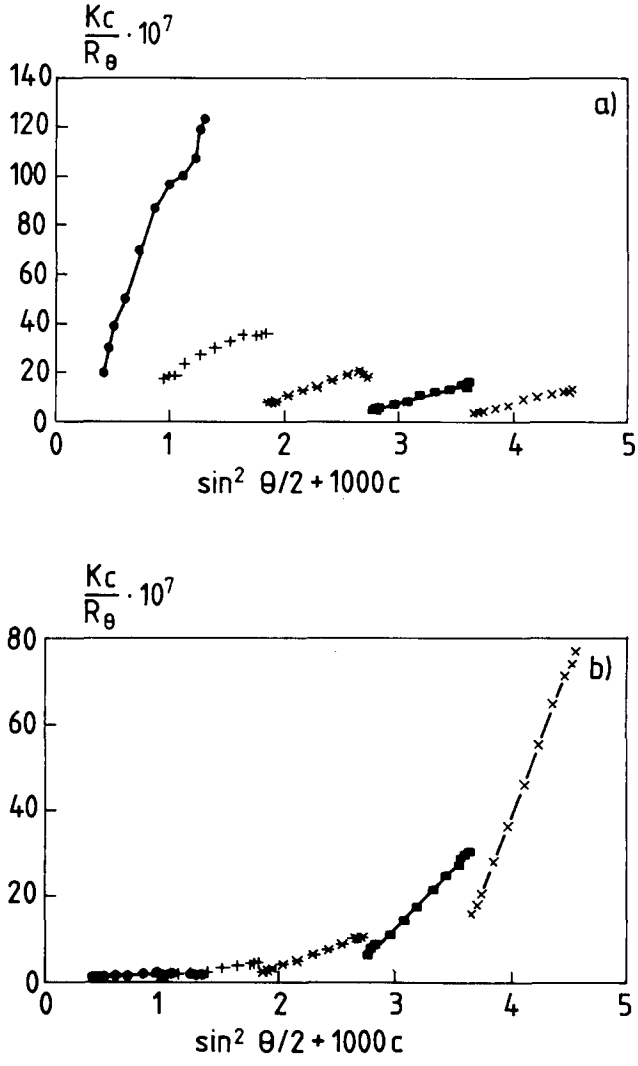

Fig. 4. Zimm plots obtained after filtering a citrus pectin series through one filter in the order of (a) increasing and (b) decreasing concentration; pore size: 0·45 μm.

$$\frac{R_\theta}{K \cdot c} = x_1 M_{W_1} P_1(\theta) + x_2 \langle M \rangle_{W_2} P_2(\theta), \qquad (6)$$

(coli) (spheres)

where x_i, M_{W_i} and $P_i(\theta)$ are the mass fraction, weight average molecular mass and the intraparticular scattering function of the two components ($i = 1, 2$). Describing the polydispersity of the components by a normalized mass distribution function $P_{W_i}(M)$ we obtain:

$$M_W = \int_0^\infty M p_W(M)\, dM \qquad (7)$$

and

$$P_z(\theta) = \frac{1}{M_W} \int_0^\infty M P(\theta, M) p_W(M)\, dM. \qquad (8)$$

The molecularly dispersed component can be simulated by Gaussian coils with the intraparticular scattering function:

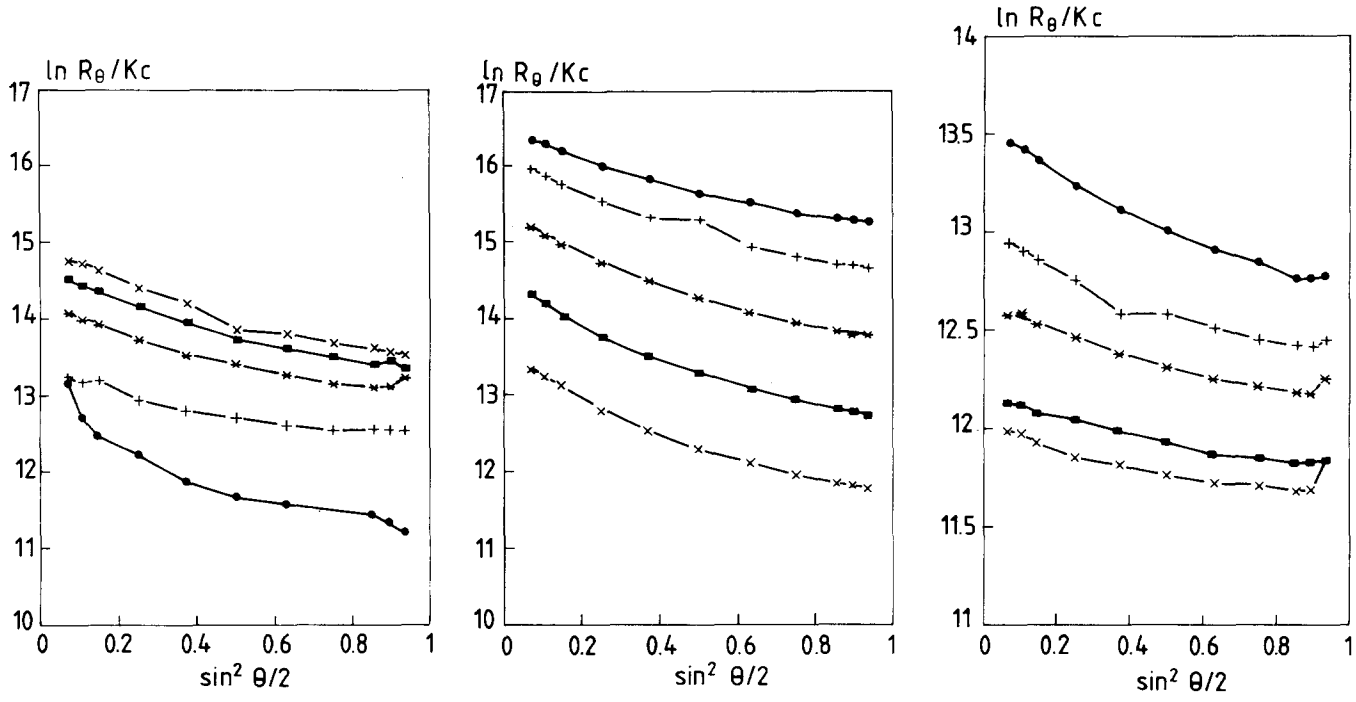

Fig. 5. Guinier plots corresponding to Fig. 4 (a) and (b) and Fig. 2 without shifting along x-axis.

$$P(\theta) = \frac{2}{u^2}[e^{-u} - 1 + u]. \tag{9}$$

where $u = q^2 s^2$ (s = radius of gyration, $q = (4\pi/\lambda)\sin(\theta/2)$) and λ = wavelength in the medium.

Using a Schulz–Zimm distribution for the polydispersity:

$$p_W(M) = \frac{y^{z+1}}{\Gamma(z+1)} M^z e^{-yM}, \tag{10}$$

a closed analytical expression for $P_z(\theta)$ can be derived:

$$P_z(\theta) = \frac{2}{(1+u)\xi^2}\quad [\xi - 1 + (1 + U\xi)^{-1/u}], \tag{11}$$

where

$$\frac{1}{z} = U = \frac{M_W}{M_n} - 1, \qquad y = \frac{z+1}{M_W}, \qquad \xi = \frac{1}{1+2u}\langle s^2\rangle_z q^2.$$

As a model for the particulate component we have employed a polydisperse system of spheres. The scattering function of a sphere of homogeneous density with radius a is given by

$$P(\theta) = \left[3\frac{\sin aq - aq\sin aq}{a^3q^3}\right]^2. \tag{12}$$

To describe the polydispersity of the particulate component we used a special logarithmic distribution function of radii which permits simulation of the influence of the polydispersity on the shape of the scattering function to a greater extent than the Schulz–Zimm distribution:

$$p_W(a) = \frac{a^{-5/2}\exp[-(\ln a - \ln a_m)^2/2\delta_a^2]}{\sqrt{2\pi}\cdot\delta_a\cdot a_m^{3/2}\exp[9\delta_a/8]}. \tag{13}$$

The molecular weight and polydispersity, are given by the relations:

$$M_W = \frac{4\pi}{3}\rho N_a a_m^3 \tag{14}$$

$$M_W/M_n = e^{9\delta_a^2}, \tag{15}$$

where N_a = Avogadro's number, and ρ = average polymer packing density. Eqns (12) and (13) are substituted into eqn (8), which is then integrated numerically.

Model calculations were performed for a fixed molecularly dissolved component with the parameters $x \simeq 1$, $M_W = 1 \times 10^5$ g mol^{-1}, $z = 1$, $\langle s^2\rangle_z^{1/2} = 20$ nm with varying amounts and radius of the particulate component at moderate polydispersity ($\delta_a = 0{\cdot}3$). The results obtained are given in Figs 6 and 7. Figure 6 demonstrates that, for small amounts of spheres, the scattering contribution of the particles dominates in the small angle region, while in the wide angle range, the scattering of the molecularly dissolved polymer prevails. With increasing amounts the particles determine the scattering curve within the whole experimental range. Figure 7 illustrates the influence of the radius of the particulate component. For radii up to 100 nm the scattering curves show a normal behaviour, giving no indication of

a bimodal system. However, the molecular mass of the molecularly dispersed species, which would be determined from the curves, is strongly influenced by the presence of the particles even when their content is as low as 0·1% by weight. For higher radii the bimolarity of the system is clearly shown by the curvature of the scattering curves.

Figures 6 and 7 suggest that the experimental findings of Fig. 4 may be due to a change in the amount and radius of the particulate component. This should be exemplified for the scattering curves in Figs 4(b) and 5(b), which were obtained after filtration in the order of decreasing concentration. These scattering curves were analysed by a more sophisticated procedure (see Part II of this series) as a bimodal system. For the molecularly dispersed component we used the following parameters: $M_W = 1 \times 10^5$ g mol^{-1} (from ultracentrifugation; Harding *et al.*, 1991), $M_W/M_n = 2$, $\langle s^2\rangle_z^{1/2} = 20$ nm (cf. Berth *et al.*, 1990). The results for the particulate component are listed in Table 3.

Only the product of the mass fraction and the molecular mass $x_2 M_{W_2}$ can be determined. This changes by nearly a factor of 20 within the concentration series. The size parameters a_M and $\langle s^2\rangle_z^{1/2}$ change in opposite directions. The decrease of $x_2 M_{W_2}$ with increasing pectin concentration shows undoubtedly that an aggregation cannot be the origin of the particulate components. The result may be explained by the fact that the fresh membrane filter holds back a larger part of the particulate component, whilst with increasing loading of the filter, more and more particles are released again. During this process a 'sorting' of particles occurs, i.e. the smaller ones (or fragments of the larger ones) are preferentially rinsed into the solution. Assuming only slight changes in the compactness of the particles, a decrease of M_{W_2} with decreasing particle size has to be expected. Therefore, the change of $x_2 M_{W_2}$ is mainly caused by a variation in x_2, which should be even greater than that indicated in column 5 of Table 3 and can be better assessed from $x_2\rho_2$ (about a factor of 100).

With the parameters of the molecularly dissolved and the particulate components given in Table 3 the scattering curves were recalculated according to eqns (6)–(13). The results are shown as Zimm plots in Fig. 8(a) and as Guinier plots in Fig. 8(b). The agreement with the experimental curves is nearly perfect, confirming convincingly, the manipulation of the particulate component during filtration could account for the observed experimental data.

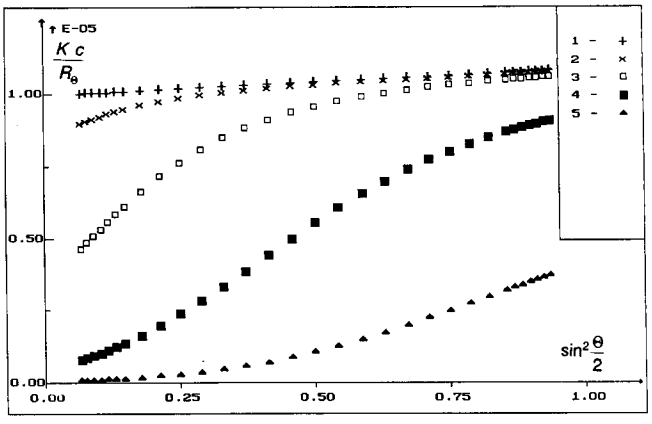

Fig. 6. Zimm plot of the scattering curves of a mixture of Gaussian coils ($M_W = 1 \times 10^5$ g/mol, $z = 1$, $\langle s^2\rangle_z^{1/2} = 20$ nm) and different small amounts of spheres ($a_m = 200$ nm, $\delta_a = 0{\cdot}3$, $\rho = 0{\cdot}1$ g/ml): 1, $x_2 = 0$; 2, $x_2 = 1 \times 10^{-5}$; 3, $x_2 = 1 \times 10^{-4}$; 4, $x_2 = 10^{-3}$; 5, $x_2 = 10^{-2}$.

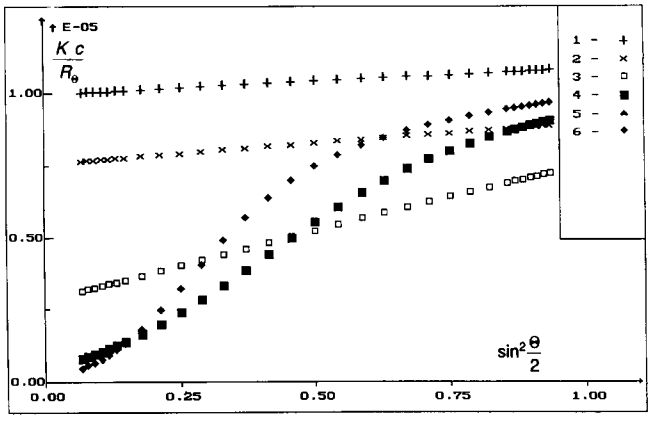

Fig. 7. Zimm plot of the scattering curves of a mixture of Gaussian coils (see Fig. 6) and spheres of different radii ($x = 1 \times 10^{-3}$, $\delta_n = 0{\cdot}3$): 1, Gaussian coils; 2, $a_m = 50$ nm; 3, $a_m = 100$ nm; 4, $a_m = 200$ nm; 5, $a_m = 300$ nm.

Table 3. Structural parameters of the particulate component estimated from the scattering curves in Fig. 4(b)/5(b)

Curve no.	δ_a	a_m	$\langle s^2\rangle_z^{1/2\,a}$	$x_2 M_{W_2} 10^{-6}$	$x_2\rho_2$
1	0·4	79	92	13·5	$1{\cdot}1 \times 10^{-2}$
2	0·4	90	104	9·5	$5{\cdot}2 \times 10^{-3}$
3	0·4	93	108	4·3	$2{\cdot}1 \times 10^{-3}$
4	0·4	110	127	1·9	$5{\cdot}7 \times 10^{-4}$
5	0·3	141	137	0·70	$9{\cdot}9 \times 10^{-5}$

$^a\langle s^2\rangle_z^{1/2} = \sqrt{\frac{3}{5}}\, a_m \cdot e^{2/5\delta_n^2}$.

CONCLUSIONS

These findings are in some conflict with our former idea of membrane filtration where membrane filters were assumed to have sharp cut-off borders, high selectivity and constant separation properties. Therefore, a more detailed consideration of filtration effects seems to be required and this will be the subject of Part II of this series. In part III we will deal with the problems of

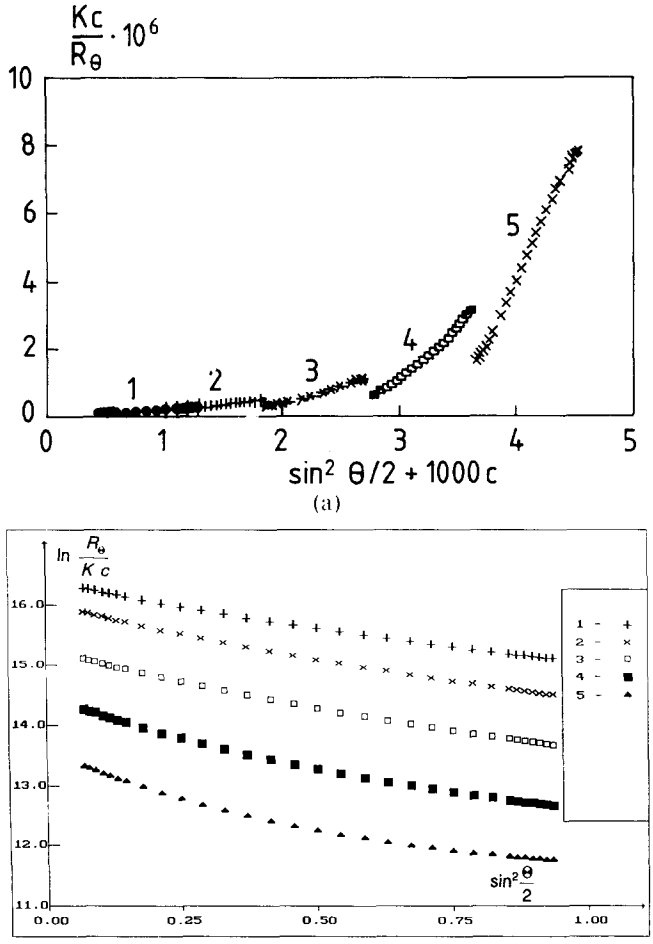

Fig. 8. Results of model calculations for a biomodal system consisting of Gaussian coils with $M_w = 1 \times 10^5$ g/mol. Zimm plot of the scattering curves of a mixture of $<s^2> = 20$ nM and particulate matter according to Table 3: (a) Zimm plot; (b) Guinier plot.

association after treatment of samples to prevent artefacts due to clarification and by using a more sophisticated interpretation of light scattering data (Dautzenberg & Rother, 1988, 1992).

ACKNOWLEDGEMENT

We thank Mrs Evelyn Lück in Potsdam-Rehbrücke for her careful laboratory assistance.

REFERENCES

Berth, G. (1988). *Carbohydr. Polym.*, **8**, 105–18.
Berth, G. (1992). *Carbohydr. Polym.*, **19**, 1–9.
Berth, G., Dautzenberg, H., Lexow, D. & Rother, G. (1990). *Carbohydr. Polym.*, **12**, 39–59.
Berth, G. & Lexow, D. (1991). *Carbohydr. Polym.*, **15**, 51–66.
Dautzenberg, H. & Rother, G. (1988). *J. Polym. Sci., Part B. Polym. Phys.*, **26**, 353–66.
Dautzenberg, H. & Rother, G. (1992). *Makromol. Chem., Makromol. Symp.*, **61**, 94–113.
Devine, W.C. (1974). Physico-chemical studies on pectins, PhD Thesis, University of Edinburgh, UK.
Evans, J.M. (1972). In *Light Scattering from Polymer Solutions*, ed. M.B. Huglin. Academic Press, London, New York, pp. 90–1.
Harding, S.E., Berth, G., Ball, A., Mitchell, J.R. & Torre, G. de la (1991). *Carbohydr. Polym.*, **16**, 1–15.
Hourdet, D. & Muller, G. (1991). *Carbohydr. Polym.*, **16**, 113–35.
Huglin, M.B. (ed.) (1972). *Light Scattering from Polymer Solutions*, Academic Press, London, New York.
Kerker, M. (1969). *The Scattering of Light and Other Electromagnetic Radiation*, Academic Press, New York, San Francisco, London.
Kratochvil, P. (1972). In *Light Scattering from Polymer Solutions*, ed. M.B. Huglin. Academic Press, London, New York, p. 371.
Pals, D.T.F. & Hermans, J.J. (1952). *Recueil*, **71**, 433–57.
Säverborn, S. (1945). *A Contribution to the Knowledge of the Acid Polyuronides*, Almquist & Wiksell, Uppsala, Sweden.
Smith, J.E. (1976). The molecular weights of pectins. PhD Thesis. University of Leeds, UK.
Tabor, B.E. (1972). *Light Scattering from Polymer Solutions*, ed. M.B. Huglin. Academic Press, London, New York, pp. 1–25.
Zimm, B.H. (1948). *J. Chem. Phys.*, **16**, 1099–116.